Structural investigation of Np_2Co_{17} and analogue compounds under pressure

A. Hen,[1,2] S. Heathman,[1] R. Eloirdi,[1] J.-C. Griveau,[1] S. Elgazzar,[3] P. M. Oppeneer,[4] I. Halevy,[2,5] I. Orion,[2] and R. Caciuffo[1]

[1]*European Commission, Joint Research Centre, Institute for Transuranium Elements, Postfach 2340, D-76125 Karlsruhe, Germany*

[2]*Nuclear Engineering Department, Ben Gurion University, Beer-Sheva, Israel*

[3]*Department of Physics, University of Johannesburg, P.O. Box 524, Auckland Park 2006, South Africa*

[4]*Department of Physics and Astronomy Uppsala University, Box 516, S-751 20 Uppsala, Sweden*

[5]*Physics Department, Nuclear Research Center Negev, P.O. Box 9001, Beer-Sheva, Israel*

(Received 25 March 2014; revised manuscript received 5 June 2014; published 13 August 2014)

The structural behavior of Np_2Co_{17} is investigated by means of high-pressure diamond-anvil compression measurements and is compared with that of the isostructural compounds Lu_2Co_{17} and Lu_2Ni_{17}. The Th_2Ni_{17}-type hexagonal crystal structure is preserved with no measurable discontinuous volume collapses up to the highest achieved pressure, $p = 43$ GPa. For Np_2Co_{17}, fits to the Birch-Murnaghan and Vinet equations of state give values of the isothermal bulk modulus and its pressure derivative of $B_0 = 286$ GPa and $B_0' = 3$, revealing that this Np compound is a highly incompressible solid with stiffness comparable to that of superhard covalently bonded materials. For the Lu_2T_{17} (T = Co, Ni) compounds, the measured bulk modulus changes from $B_0 = 137$ GPa for T = Co to $B_0 = 257$ GPa for T = Ni. The isothermal equation of state for the studied compounds are in excellent agreement with the results of *ab initio* fully relativistic, full-potential local spin-density functional calculations. Theoretical estimates of the bulk modulus are given also for Np_2Ni_{17}, for which B_0 is predicted to assume values intermediate between those measured for Lu_2Ni_{17} and Np_2Co_{17}.

DOI: 10.1103/PhysRevB.90.054107 PACS number(s): 71.27.+a, 78.70.Nx, 75.30.Et

I. INTRODUCTION

Np_2Co_{17} is a transuranic analog of the widely investigated Sm_2Co_{17} high-performance permanent magnet [1,2]. It crystallizes in the $P6_3/mmc$ (D_{6h}) space group with the Th_2Ni_{17}-type hexagonal structure. The unit cell is composed of 38 atoms with the Np atoms residing at 2*b* and 2*d* special positions, and the Co atoms at the 4*f*, 6*g*, 12*k*, and 12*j* sites. The two Np sites have a similar Co nearest-neighbor environment but a different nearest Np coordination. However, crystallographic disorder, which is not uncommon for the rare earths analogues [3], may contribute to average the differences in the close surrounding of the two Np sites.

The magnetic properties of Np_2Co_{17} have been recently investigated on the basis of magnetization, Mössbauer, and x-ray magnetic circular dichroism measurements [4]. Magnetization curves indicate the occurrence of ferromagnetic order below a $T_C > 350$ K. Mössbauer spectra suggest a Np^{3+} oxidation state and give an ordered moment of $\mu_{Np} = 1.57(4)\ \mu_B$ and $\mu_{Np} = 1.63(4)\ \mu_B$ for the Np atoms located, respectively, at the 2*b* and 2*d* crystallographic positions. Combining these values with a sum rule analysis of the XMCD spectra measured at the neptunium $M_{4,5}$ absorption edges, the spin and orbital contributions to the site-averaged Np moment ($\mu_S = -1.88(9)\ \mu_B$, $\mu_L = 3.48(9)\ \mu_B$) have been determined. The ordered moment averaged over the four inequivalent Co sites, as obtained from the saturation value of the magnetization, is $\mu_{Co} \simeq 1.6\ \mu_B$.

Lu_2T_{17} (T = Co and Ni) also crystallize in the Th_2Ni_{17}-type hexagonal structure and are both ferromagnetic. The Co compound orders at $T_C = 1210$ K and exhibits a spontaneous magnetic moment at 5 K of 27.6 μ_B per formula unit (1.6 μ_B per Co atom). A spin reorientation from easy-plane to easy-axis type of magnetic anisotropy is observed at 740 K [5]. Lu_2Ni_{17} has a T_C of about 600 K and a Ni moment of 0.27 μ_B, suggesting that almost all Lu valence electrons are transferred to the Ni 3*d* band [6].

Here we report x-ray diffraction diamond-anvil cell (DAC) compression studies to 43 GPa for Np_2Co_{17} and its isostructural analogues Lu_2Co_{17} and Lu_2Ni_{17}. We have measured the isothermal equation of state (EOS) and the ratio c/a between the two lattice parameters defining the hexagonal unit cell. Using the third-order Birch-Murnaghan EOS [7–9] or the analytic approximation to the Vinet EOS [10] to fit the data, we have found that the bulk modulus B_0 increases from 137 GPa in Lu_2Co_{17} to 286 GPa in Np_2Co_{17}. The latter value is among the highest reported for an intermetallic compound [11]. The bulk modulus we obtained for Lu_2Ni_{17} is $B_0 = 257$ GPa, about 80% larger than for the Co analog and about 70% larger than for Er_2Fe_{17} [12]. We have not been able to measure the compressibility of Np_2Ni_{17}, but *ab initio* calculations based on the local spin-density approximation (LSDA) do not predict a similar increase of B_0 if Ni is substituted for Co in Np_2Co_{17}.

The remainder of this paper is structured as follows. In Sec. II, we provide details on synthesis and experimental procedures; in Sec. III we present the experimental results and the fits to phenomenological EOS, whereas the results of first-principles electronic-structure calculations are presented in Sec. IV. A short summary and conclusions are found in Sec. V.

II. EXPERIMENTAL DETAILS

Polycrystalline samples of Np_2Co_{17} and Lu_2T_{17} were prepared by arc melting stoichiometric amounts of high-purity elemental constituents (99.9% Np, 99.9% Lu, 99.999% Co and

Ni) on a water-cooled copper hearth, under Ar (99.9999%) atmosphere. A Zr alloy was used as an oxygen getter. The weight losses during melting were less than 0.2%. The samples were melted five times to improve the homogeneity, then wrapped in tantalum foils, and annealed at 800 °C in evacuated quartz ampoules for 1 week. Phase analysis of the obtained ingots was performed before and after annealing. Crystallographic analyses were performed at room temperature by x-ray diffraction on samples with a mass of about 25 mg, ground, and dispersed on a Si wafer. Data were collected in back-reflection mode with a Bruker D8 diffractometer installed inside a α-γ glove box, using Cu-Kα_1 radiation selected by a Ge (111) monochromator. A 1D position sensitive detector was used to cover the angular range from 15 to 120 degrees, with incremental steps of 0.0085 degrees.

About 10 μg of material were loaded into a membrane-type diamond anvil cell (DAC), affording a maximum x-ray scattering angle $2\theta_{max} \approx 36°$. Diamond culets were of 500-μm diameter with preindented inconel gaskets of 200-μm (diameter) hole and (indented) thickness 30 μm. Pressure was calibrated by the ruby fluorescence method, using a single ruby-ball of diameter smaller than 10 μm. To avoid the risk of contamination of any exterior part of the DAC, the Np_2Co_{17} powders were combined with a small amount of epoxy resin to form solid ("granular") pieces, which were loaded into the DAC. Sample loading of the DAC was done in inert atmosphere inside a glove box to protect the sample from moisture and air, as well as to provide confinement for the radioactive material. Safety regulations impose sealing the DAC by application of a finite pressure p_{min} before removal to the x-ray diffractometer. For this reason, diffraction patterns for pressures smaller than p_{min} cannot be recorded. In this study, $p_{min} = 4.3$ GPa. Attention must also be paid to the pressure-transmitting medium being used, to assure that it will not cause sample degradation (alcohol, for instance, in presence of a high radiation field in a confined space can be decomposed to aggressive products), or risks of radioactive contamination upon decompression (for instance in the case of liquefied gases such as Ar or N_2). A common choice in high-pressure studies of transuranium materials is to use silicone oil, although it is known that a quasihydrostatic behavior with this medium is achieved only in a restricted pressure range [13]. This fact has been taken into account in the data analysis, as reported below.

Measurements were performed at ITU, Karlsruhe, from 4.3 up to 43 GPa using a modified Bruker D8 x-ray diffractometer with focusing mirror optics installed on a Bruker molybdenum rotating anode x-ray source. X-ray wavelength and spot-size at the sample position were 0.70926 Å (Mo Kα_1) and 100 $\times$ 100 μm^2. Diffraction images were recorded with a Bruker SMART Apex II charge-coupled device (CCD), 1024 $\times$ 1024 pixels of dimensions 61 $\times$ 61 μm^2. The DAC was rotated through a sample angle $\Delta\Omega = \pm 4°$ while collecting each diffraction image. The DAC to sample distance and CCD nonorthogonality corrections were calibrated using powder diffraction from a LaB_6 standard. The images were integrated using the ESRF FIT2D software [14], which generates files suitable for profile refinement. Rietveld and Le Bail refinement techniques have been used to determine the variation of the lattice parameters with increasing pressure.

Vickers microhardness measurements have been performed with a Leitz *miniload 2* durometer put inside a α-γ glove box. For these measurements we also prepared samples of the isostructural compounds Np_2Ni_{17}. Indentation was performed by applying a load of 200 N to polished samples having a flat surface of about 20 mm^2. Hardness values have been obtained by averaging the results of nine independent measurements for each sample.

III. EXPERIMENTAL RESULTS

The ambient-pressure powder diffraction pattern of Np_2Co_{17} is shown as an example in Fig. 1. The Rietveld analysis was performed with the X'Pert HighScore Plus software package of PANalytical. The background was fitted with a polynomial, and the shape of the Bragg peaks was described by a pseudo-Voigt function. The observed Bragg peaks for all three investigated compounds can be indexed in the hexagonal $P6_3/mmc$ space group, with lattice parameters given in Table I. The best fit was obtained assuming full occupation of the sites corresponding to the ideal Th_2Ni_{17}-type of structure. The structural parameters are also reported in Table I. The crystal structure, shown in the inset of Fig. 1, consists of three different planes stacked perpendicularly to the c axis in the sequence ABAC. Planes A contain Co (Ni) atoms located at 6g and 12k positions, planes B and C contain both 12j Co (Ni) atoms and Np (Lu) at 2b and 2d sites. The transition metal atoms at 4f positions form a dumbbell arrangement separating A, B, and C planes.

Examples of angle-dispersive x-ray diffraction results for Np_2Co_{17} at different applied pressures are shown in Fig. 2, whereas an example of profile-fitted diffraction data is shown in Fig. 3. Peak broadening did not affect the quality of the refinements up to 30 GPa. For higher pressure, some principal

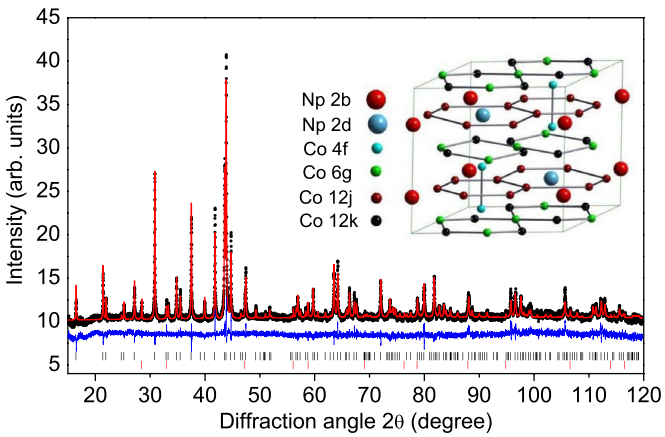

FIG. 1. (Color online) Observed (dots) and calculated (red line) x-ray diffraction pattern recorded at room temperature and ambient pressure for Np_2Co_{17}. The lower trace (blue line) is the difference profile. The intensity distribution is plotted as a function of the full diffraction angle 2θ (Cu Kα_1 radiation). Vertical ticks indicate calculated angular positions of the Bragg peaks for (upper row, black) the Np_2Co_{17} phase and (lower row, red) for an impurity phase (NpO_2, ~3% in weight). The inset shows the crystal structure of Np_2Co_{17}, corresponding to the ABAC stacking sequence characteristic of the ordered Th_2Ni_{17}-type structure.

TABLE I. Refined structural parameters for Np_2Co_{17} and Lu_2Ni_{17}, at room temperature and ambient pressure. The parameters are referred to the hexagonal axes (space group $P6_3/mmc$). Full occupation were assumed for all sites. Np(Lu) atoms reside at $2b(\bar{6}m2,00\ 1/4)$ and $2d(\bar{6}m2,1/32/3\ 3/4)$ sites; $Co_2(Ni_2)$ reside at the $6g(2/m,1/20\ 0)$ site. The lattice parameters obtained at room temperature for Lu_2Co_{17} are $a = 8.2529(2)$ Å and $c = 8.1060(5)$ Å.

Atom	Site	x	y	z
Np_2Co_{17}	$a = 8.3107(1)$ Å		$c = 8.1058(1)$ Å	
Co_1	$4f$	1/3	2/3	0.1048(5)
Co_3	$12j$	0.3241(5)	0.9547(3)	1/4
Co_4	$12k$	0.1663(3)	0.3326(6)	0.9775(3)
Lu_2Ni_{17}	$a = 8.2659(1)$ Å		$c = 8.0278(9)$ Å	
Ni_1	$4f$	1/3	2/3	0.1094(3)
Ni_3	$12j$	0.3279(3)	0.9594(2)	1/4
Ni_4	$12k$	0.1657(1)	0.3315(3)	0.9810(2)

reflections become masked by gasket peaks and the spectrum quality deteriorates. The hexagonal ambient-pressure crystallographic structure is preserved over the investigated pressure range, the lattice being compressed continuously.

The experimental isotherm EOS for the three compounds is shown in Fig. 4. The results have been fitted with a third-order Birch-Murnaghan EOS [7–9],

$$p(V) = \frac{3}{2}B_0\left[\left(\frac{V}{V_0}\right)^{-\frac{7}{3}} - \left(\frac{V}{V_0}\right)^{-\frac{5}{3}}\right] \times \left\{1 + \frac{3}{4}(B_0' - 4)\left[\left(\frac{V}{V_0}\right)^{-\frac{2}{3}} - 1\right]\right\}, \quad (1)$$

where p is the applied pressure, V_0 is the ambient-pressure unit cell volume, B_0 is the isothermal bulk modulus, and B_0' its

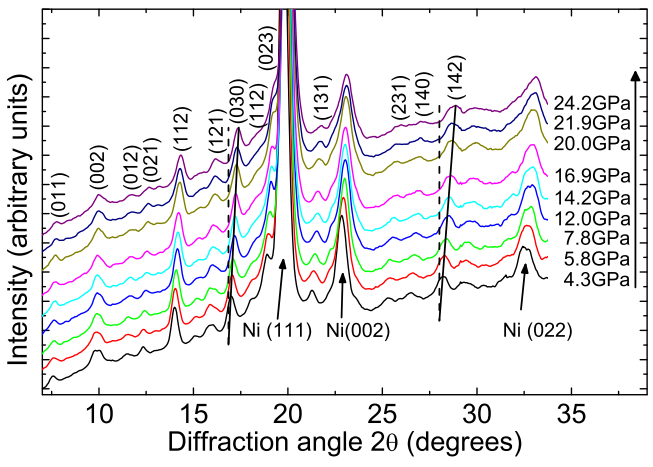

FIG. 2. (Color online) Diffraction patterns of Np_2Co_{17} for selected pressures at room temperature, obtained by integrating Debye-Scherrer rings recorded with the area detector. Patterns are offset vertically for clarity. No splitting of Bragg peaks or extra reflections appear with increasing pressure. The values of the lattice parameters decrease continuously, as indicated by the tilted straight lines. Nickel Bragg peaks from the inconel gasket are indicated by arrows. Full data set have been collected up to 43 GPa.

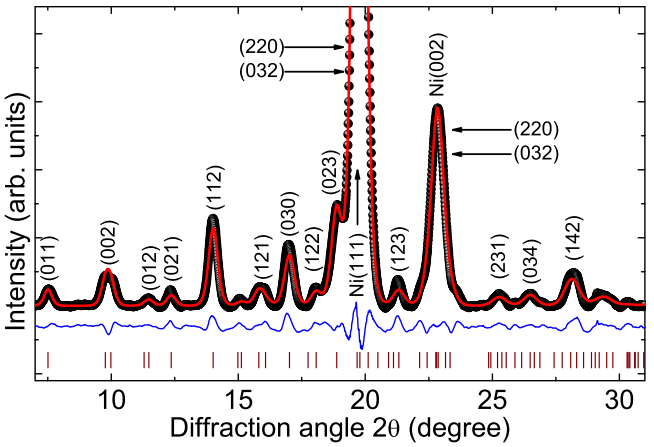

FIG. 3. (Color online) Diffraction pattern obtained for Np_2Co_{17} inside a membrane-type diamond anvil cell and submitted to a pressure of 4.3 GPa using silicone oil as pressure transmitting medium. Black circles represent experimental data, the solid red line is the refined Le Bail profile, vertical lines are reflection tick marks, and the lower blue line represents the difference profile. Nickel Bragg peaks are due to the inconel gasket.

pressure derivative. The resulting fits are shown by solid lines in Fig. 4 and give $B_0 = (286 \pm 5)$ GPa and $B_0' = 3$ for Np_2Co_{17}, $B_0 = (137 \pm 1)$ GPa and $B_0' = 5$ for Lu_2Co_{17}, and $B_0 = (257 \pm 2)$ GPa and $B_0' = 2.5$ for Lu_2Ni_{17}. As mentioned before, silicone oil has a quasihydrostatic behavior only in a restricted pressure range. For this reason, the fits have been performed using data in different pressure intervals, first up to 14 GPa and then up to 32 GPa. The difference between the values for the fitted parameters in the two cases determines the quoted experimental uncertainties. In the case of the Lu compounds, two independent diffraction data sets have been collected, obtaining the same results within experimental errors.

As an alternative approach to determine the bulk modulus for the three samples, the analytic approximation to the Vinet

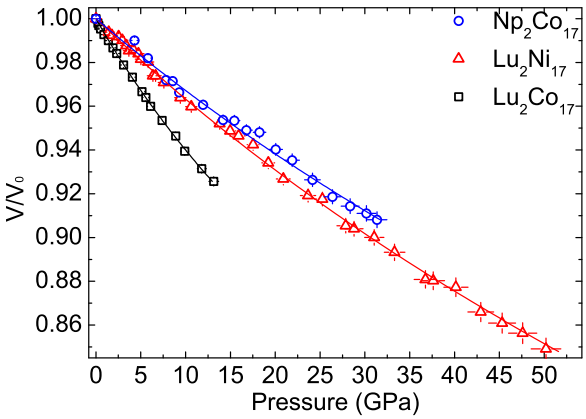

FIG. 4. (Color online) Experimental isothermal equation of state for Np_2Co_{17}, Lu_2Co_{17}, and Lu_2Ni_{17}. The normalized unit cell volume, $V(p)/V_0$, is plotted as a function of applied pressure. The solid lines through experimental data are fit to the third-order Birch-Murnaghan equation of state. Error bars are derived from refinement.

TABLE II. Bulk modulus and derivative obtained for the three investigated samples by fitting experimental compression curves to different phenomenological equations of state.

	Birch-Murnaghan		Vinet	
	B_0 (GPa)	B_0'	B_0 (GPa)	B_0'
Np_2Co_{17}	286 ± 5	3	285 ± 5	3
Lu_2Co_{17}	137 ± 1	5	137 ± 1	5
Lu_2Ni_{17}	257 ± 2	2.5	255 ± 6	2.5

EOS [10] was also used:

$$p(V) = 3B_0 \frac{1 - f_V}{f_V^2} \exp\left[\frac{3}{2}(B_0' - 1)(1 - f_V)\right], \qquad (2)$$

where $f_V = (V/V_0)^{1/3}$. The results of the two approaches are fully consistent (see Table II).

IV. *AB INITIO* CALCULATIONS AND COMPARISON WITH EXPERIMENTAL RESULTS

Ab initio density-functional theory calculations were performed with the relativistic version [15] of the full potential local orbital method (RFPLO) [16]. In this scheme the four-component Kohn-Sham-Dirac equation, which implicitly contains spin-orbit coupling up to all orders, is solved self-consistently. The Perdew-Wang parametrization of the exchange-correlation (XC) potential in LSDA was used [17]. The adopted set of valence basis states was $5f$; $6s6p6d$; $7s7p$ for Np, $4f$; $5s5p5d$; $6s6p$ for Lu, and $3d$; $4s4p$ for Co and Ni. The ground state properties have been calculated assuming a nonmagnetic configuration. The self-consistent determination of the Np $5f$ occupancy number led to a value of 3.8, supporting the assumption that Np ions in Np_2T_{17} are practically trivalent.

Total energy calculations were performed as a function of volume, for a $10 \times 10 \times 10$ **k** mesh, corresponding to 84 **k** vectors in the irreducible wedge of the tetragonal Brillouin zone. The unit cell contains 38 atoms. The volume dependence of the cohesive energy $E(V)$ is then obtained from the total energies by subtracting isolated atom contributions. The equation of state at 0 K is finally calculated from the variation of the cohesive energy with respect to volume, $P = -\partial E/\partial V$, and is compared to experimental values in Fig. 5. We note that the experimental compressibility curves have been obtained at room temperature. The experimental volume differs, therefore, from the zero-temperature volume by the effect of the thermal expansion, which is neglected. This is a good approximation, because we consider the relative volume, $V(p)/V_0$, in which the thermal expansion is practically canceled. Experimental and theoretical values for the bulk modulus and its first pressure derivative are compared in Table III.

V. DISCUSSION AND CONCLUSIONS

The results reported above reveal that Lu_2Ni_{17} has a bulk modulus about twice as large as the isostructural compound Lu_2Co_{17} and falls under the less compressible intermetallics [11,18]. The large variation observed between the two compounds is surprising, for empirical models would rather predict a similar value for their bulk modulus B_0 [11,18]. The most striking difference between the two compounds concerns their magnetic properties. Both are ferromagnetic, but the Co atoms in Lu_2Co_{17} carry on average a magnetic moment that is about a factor six larger than the average Ni magnetic moment in Lu_2Ni_{17}. This suggests that the Ni $3d$ band is almost filled, so that the valence electron density at the transition metal site is larger in the nickel compound. A larger valence electron density usually leads to a higher bulk modulus. Np_2Co_{17} has also a B_0 more than twice as large as Lu_2Co_{17}, with a value approaching that of stishovite (291 GPa, Ref. [19]) and cubic BN (369 GPa, Ref. [20]). However, the Co sublattice in the Np and Lu analogs has essentially the same magnetization. In this case, the difference in B_0 could be due to the participation to bonding of the partially localized Np $5f$ electrons [4].

TABLE III. Comparison of experimental and *ab initio* calculated bulk modulus (B_0) and its pressure derivative (B_0') of Np_2T_{17} and Lu_2T_{17} (T = Co, Ni). H_V is the Vickers microhardness, in GPa units, obtained with an applied load of 200 N for polycrystalline samples.

	Experiment			Theory	
	B_0 (GPa)	B_0'	H_V	B_0 (GPa)	B_0'
Np_2Co_{17}	286(5)	3	6.5(5)	285	4.9
Lu_2Co_{17}	137(1)	5	6.8(3)	135	7.3
Np_2Ni_{17}	–	–	5.8(3)	274	4.6
Lu_2Ni_{17}	257(2)	2.5	7.1(3)	254	4.9

First-principles simulations for Np_2Ni_{17} do not predict an increase of B_0 as the one observed for Lu_2T_{17} upon substitution of Co for Ni. For technical reasons, we have not been able to perform x-ray diffraction compressibility studies for Np_2Ni_{17}. However, the agreement between theoretical predictions and experimental values for the other compounds investigated here lends credibility to the calculations, which exclude an extremely high value of B_0 for Np_2Ni_{17}. Whereas the other three compounds examined in this study are ferromagnetic above room temperature, Np_2Ni_{17} remains paramagnetic down to 17 K, where a transition to a complex antiferromagnetic phase occurs [21]. This suggests that the electronic structure of the A_2T_{17} compounds (A = Np, Lu) is very sensitive to lattice substitution. It is plausible that the Np $5f$ electrons in Np_2Ni_{17} are even more localized than in Np_2Co_{17} and do not participate substantially to bonding. This could naively explain the similar values of B_0 found for the two A_2Ni_{17}.

So far, the material with the highest known bulk modulus is osmium [22] ($B_0 = 462$ GPa), followed by diamond [23] ($B_0 = 443$ GPa), which is also the hardest known material. Indeed, in many instances, a high bulk modulus is correlated with a high mechanical hardness [24], although the first property determines the response to elastic deformations, the second one is related to the capacity of the material to resist plastic deformation. For the compounds investigated here, hardness measurements show that they are only moderately hard, with a Vickers hardness number in the range ~6–7 GPa. Table III gives the results obtained by a Vickers microhardness tester and shows that the variations of hardness

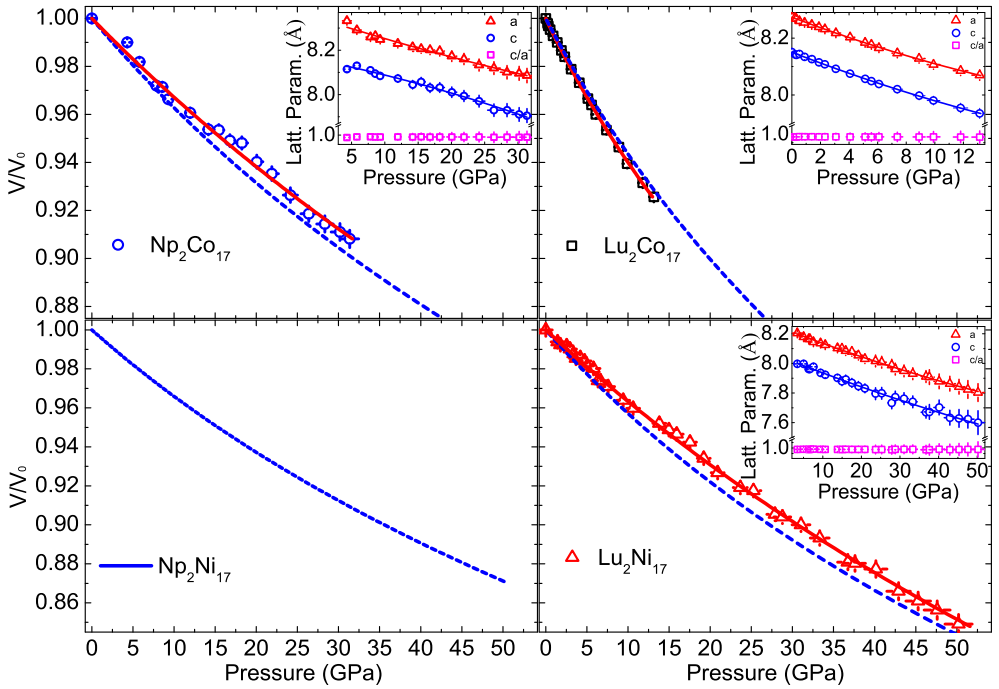

FIG. 5. (Color online) Comparison between experimental (symbols) and *ab initio* calculated compression curves of Np_2Co_{17}, Lu_2Co_{17}, and Lu_2Ni_{17}. The calculated equation of state (EOS) is shown also for Np_2Ni_{17}, for which experimental data are not available. Solid lines are fit to the Birch-Murnaghan EOS. The calculated curves are shown as blue dashed lines. Insets show the measured pressure variation of the lattice parameters a and c, and of their ratio c/a, demonstrating isotropic compression conditions.

are not correlated with compressibility, probably because of the presence of lattice defects in the indented samples.

In conclusion, the results of diamond-anvil cell x-ray diffraction compression studies of Np_2Co_{17} show that this compound is characterized by a very large bulk modulus, whose value approaches those of the least compressible known materials. The B_0 value measured for Np_2Co_{17} is about twice as large as the one measured for the isostructural compound Lu_2Co_{17} but comparable to the value measured for Lu_2Ni_{17}. First-principles electronic structure calculations reproduce well the equation of state experimentally determined for Np_2Co_{17} and Lu_2T_{17}. These calculations predict for Np_2Ni_{17} a value of B_0 close to the one obtained for the Lu analog. The four compounds are moderately hard and, despite the large differences in their bulk modulus, have polycrystalline Vickers microhardness of comparable value.

ACKNOWLEDGMENTS

We thank D. Bouëxière, G. Pagliosa, F. Bocci, and C. Boshoven for their technical support. The high purity neptunium metal required for the fabrication of the sample was made available through a loan agreement between Lawrence Livermore National Laboratory and ITU, in the frame of a collaboration involving LLNL, Los Alamos National Laboratory, and the US Department of Energy. A.H. acknowledges the European Commission for support in the frame of the Training and Mobility of Researchers programme.

[1] K. Kumar, J. Appl. Phys. **63**, R13 (1988).
[2] J. M. D. Coey, *Rare-Earth Iron Permanent Magnets* (Clarendon Press, Oxford, 1996).
[3] O. Moze, R. Caciuffo, B. Gillon, G. Calestani, F. E. Kayzel, and J. J. M. Franse, Phys. Rev. B **50**, 9293 (1994).
[4] I. Halevy, A. Hen, I. Orion, E. Colineau, R. Eloirdi, J.-C. Griveau, P. Gaczyński, F. Wilhelm, A. Rogalev, J.-P. Sanchez, M. L. Winterrose, N. Magnani, A. B. Shick, and R. Caciuffo, Phys. Rev. B **85**, 014434 (2012).
[5] E. A. Tereshina and A. V. Andreev, Intermetallics **18**, 641 (2010).
[6] P. D. Carfagna, J. Appl: Phys. **39**, 5259 (1968).
[7] F. Murnaghan, Am. J. Math. **59**, 235 (1937).
[8] F. Birch, J. Appl. Phys. **9**, 279 (1938).
[9] F. Birch, Phys. Rev. **71**, 809 (1947).
[10] P. Vinet, J. R. Smith, J. Ferrante, and J. H. Rose, Phys. Rev. B **35**, 1945 (1987).
[11] C. Li and P. Wu, Chem. Mater. **13**, 4642 (2001).
[12] P. Álvarez-Alonso, P. Gorria, J. A. Blanco, J. Sánchez-Marcos, G. J. Cuello, I. Puénte-Orench, J. A. Rodríguez-Velamazán, G. Garbarino, I. de Pedro, J. R. Fernández, and J. L. Sánchez Llamazares, Phys. Rev. B **86**, 184411 (2012).
[13] S. Klotz, J.-C. Chervin, P. Munsch, and G. Le Marchand, J. Phys. D: Appl. Phys. **42**, 075413 (2009).
[14] A. P. Hammersley, S. O. Svensson, M. Hanfland, A. N. Fitch, and D. Haüsermann, High Press. Res. **14**, 235 (1996).

[15] H. Eschrig, M. Richter, and I. Opahle, in *Relativistic Electronic Structure Theory—Part II: Applications*, edited by P. Schwerdtfeger (Elsevier, Amsterdam, 2004), pp. 723–776.
[16] K. Koepernik and H. Eschrig, Phys. Rev. B **59**, 1743 (1999).
[17] J. P. Perdew and Y. Wang, Phys. Rev. B **45**, 13244 (1992).
[18] C. Li, Y. L. Chin, and P. Wu, Intermetallics **12**, 103 (2004).
[19] J. M. Léger, Nature **383**, 401 (1996).
[20] C. M. Sung and M. Sung, Mater. Chem. Phys. **43**, 1 (1996).
[21] A. Hen *et al.* (unpublished).
[22] H. Cynn, J. E. Klepeis, C.-S. Yoo, and D. A. Young, Phys. Rev. Lett. **88**, 135701 (2002).
[23] H. J. McSkimin and W. L. Bond, Phys. Rev. **105**, 116 (1957).
[24] L. S. Dubrovinsky, N. A. Dubrovinskaia, V. Swamy, J. Muscat, N. M. Harrison, R. Ahuja, B. Holm, and B. Johansson, Nature **410**, 653 (2001).